arXiv:1909.06473v2 [eess.IV] 1 Dec 2019

Learned imaging with constraints and uncertainty quantification

Felix J. Herrmann, Ali Siahkoohi, and Gabrio Rizzuti
School of Computational Science and Engineering
Georgia Institute of Technology
{felix.herrmann, alisk, rizzuti.gabrio}@gatech.edu

Abstract

We outline new approaches to incorporate ideas from deep learning into wave-based least-squares imaging. The aim, and main contribution of this work, is the combination of handcrafted constraints with deep convolutional neural networks, as a way to harness their remarkable ease of generating natural images. The mathematical basis underlying our method is the expectation-maximization framework, where data are divided in batches and coupled to additional "latent" unknowns. These unknowns are pairs of elements from the original unknown space (but now coupled to a specific data batch) and network inputs. In this setting, the neural network controls the similarity between these additional parameters, acting as a "center" variable. The resulting problem amounts to a maximum-likelihood estimation of the network parameters when the augmented data model is marginalized over the latent variables.

1 The seismic imaging problem

In least-squares imaging, we are interested in inverting the following inconsistent ill-conditioned linear inverse problem:

$$\underset{x}{\text{minimize}}\, \frac{1}{2} \sum_{i=1}^{N} \|y_i - A_i x\|_2^2. \tag{1}$$

In this expression, the unknown vector x represents the image, $y_i,\ i = 1, \ldots, N$ the observed data from N source experiments and A_i the discretized linearized forward operator for the ith source experiment. Despite being overdetermined, the above least-squares imaging problem is challenging. The linear systems A_i are large, expensive to evaluate, and inconsistent because of noise and/or linearization errors.

As in many inverse problems, solutions of problem 1 benefit from adding prior information in the form of penalties or preferentially in the form of constraints, yielding

$$\underset{x}{\text{minimize}}\, \frac{1}{2} \sum_{i=1}^{N} \|y_i - A_i x\|_2^2 \quad \text{subject to} \quad x \in \mathcal{C} \tag{2}$$

with $\mathcal{C}$ representing a single or multiple (convex) constraint set(s). This approach offers the flexibility to include multiple handcrafted constraints. Several key issues remain, namely; *(i)* we can not afford to work with all N experiments when computing gradients for the above data-misfit objective; *(ii)* constrained optimization problems converge slowly; *(iii)* handcrafted priors may not capture complexities of natural images; *(iv)* it is non-trivial to obtain uncertainty quantification information.

33rd Conference on Neural Information Processing Systems (NeurIPS 2019), Vancouver, Canada.

2 Stochastic linearized Bregman

To meet the computational challenges that come with solving problem 2 for non-differentiable structure promoting constraints, such as the ℓ_1-norm, we solve problem 2 with Bregman iterations for a batch size of one. The kth iteration reads

$$\begin{array}{rcl} \tilde{x} & \leftarrow & \tilde{x} - t_k A_k^\top (A_k x - y_k) \\ x & \leftarrow & \mathcal{P}_{\mathcal{C}}(\tilde{x}) \end{array} \tag{3}$$

with $A_k^\top$ the adjoint of A_k , where $A_k \in \{A_i\}_{i=1}^N$, and

$$\mathcal{P}_{\mathcal{C}}(\tilde{x}) = \underset{x}{\operatorname{argmin}} \frac{1}{2}\|x - \tilde{x}\|_2^2 \quad \text{subject to} \quad x \in \mathcal{C} \tag{4}$$

being the projection onto the (convex) set and $t_k = \|A_k x - y_k\|_2^2 / \|A_k^\top (A_k x - y_k)\|_2^2$ the dynamic steplength. Contrary to the Iterative Shrinkage Thresholding Algorithm (ISTA), we iterate on the dual variable $\tilde{x}$. Moreover, to handle more general situations and to ensure we are for every iteration feasible (= in the constraint set) we replace sparsity-promoting thresholding with projections that ensure that each model iterate remains in the constraint set. As reported in Witte et al. [1], iterations 3 are known to converge fast for pairs $\{y_k,\, A_k\}$ that are randomly drawn, with replacement, from iteration to iteration. As such, Equation 3 can be interpreted as stochastic gradient descent on the dual variable.

3 Deep prior with constraints

Handcrafted priors, encoded in the constraint set $\mathcal{C}$, in combination with stochastic optimization, where we randomly draw a different source experiment for each iteration of Equation 3, allow us to create high-fidelity images by only working with random subsets of the data. While encouraging, this approach relies on handcrafted priors encoded in the constraint set $\mathcal{C}$. Motivated by recent successes in machine learning and deep convolutional networks (CNNs) in particular, we follow Van Veen et al. [2], Dittmer et al. [3] and Wu and McMechan [4] and propose to incorporate CNNs as deep priors on the model. Compared to handcrafted priors, deep priors defined by CNNs are less biased since they only require the model to be in the range of the CNN, which includes natural images and excludes images with unnatural noise. In its most basic form, this involves solving problems of the following type [2]:

$$\underset{w}{\text{minimize}} \frac{1}{2}\|y - Ag(z, w)\|_2^2. \tag{5}$$

In this expression, $g(z, w)$ is a deep CNN parameterized by unknown weights w and $z \sim \mathrm{N}(0, 1)$ is a fixed random vector in the latent space. In this formulation, we replaced the unknown model by a neural net. This makes this formulation suitable for situations where we do not have access to data-image training pairs but where we are looking for natural images that are in the range of the CNN. In recent work by Van Veen et al. [2], it is shown that solving problem 5 can lead to good estimates for x via the CNN $g(z, \widehat{w})$ where $\widehat{w}$ is the minimizer of problem 5 highly suitable for situations where we only have access to data. In this approach, the parameterization of the network by w for a fixed z plays the role of a non-linear redundant transform.

While using neural nets as strong constraints may offer certain advantages, there are no guarantees that the model iterates remain physically feasible, which is a prerequisite if we want to solve non-linear imaging problems that include physical parameters [5, 6]. Unless we pre-train the network, early iterations while solving problem 5 will be unfeasible. Moreover, as mentioned by Van Veen et al. [2], results from solving inverse problems with deep priors may benefit from additional types of regularization. We accomplish this by combining hard handcrafted constraints with a weak constraint for the deep prior resulting in a reformulation of the problem 5 into

$$\underset{x \in \mathcal{C},\, w}{\text{minimize}} \frac{1}{2}\|y - Ax\|_2^2 + \frac{\lambda^2}{2}\|x - g(z, w)\|_2^2. \tag{6}$$

In this expression, the deep prior appears as a penalty term weighted by the trade-off parameter $\lambda > 0$. In this weak formulation, x is a slack variable, which by virtue of the hard constraint will be feasible throughout the iterations.

The above formulation offers flexibility to impose constraints on the model that can be relaxed during the iterations as the network is gradually "trained". We can do this by either relaxing the constraint set (eg. by increasing the size of the TV-norm ball) or by increasing the trade-off parameter λ.

4 Learned imaging via expectation maximization

So far, we used the neural network to regularize inverse problems deterministically by selecting a single latent variable z and optimizing over the network weights initialized by white noise. While this approach may remove bias related to handcrafted priors, it does not fully exploit documented capabilities of generative neural nets, which are capable of generating realizations from a learned distribution. Herein lies both an opportunity and a challenge when inverse problems are concerned where the objects of interest are generally not known a priori. Basically, this leaves us with two options. Either we assume to have access to an oracle, which in reality means that we have a training set of images obtained from some (expensive) often unknown imaging procedure, or we make necessary assumptions on the statistics of real images. In both cases, the learned priors and inferred posteriors will be biased by our (limited) understanding of the inversion process, including its regularization, or by our (limited) understanding of statistical properties of the unknown e.g. geostatistics [7]. The latter may lead to perhaps unreasonable simplifications of the geology while the former may suffer from remnant imprint of the nullspace of the forward operator and/or poor choices for the handcrafted and deep priors.

4.1 Training phase

Contrary to approaches that have appeared in the literature, where the authors assume to have access to a geological oracle [7] to train a GAN as a prior, we opt to learn the posterior through inversion deriving from the above combination of hard handcrafted constraints and weak deep priors with the purpose to train a network to generate realizations from the posterior. Our approach is motivated by Han et al. [8] who use the Expectation Maximization (EM) technique to train a generative model on sample images. We propose to do the same but now for seismic data collected from one and the same Earth model.

To arrive at this formulation, we consider each of the N source experiments with data y_k as separate datasets from which images x_k can in principle be inverted. In other words, contrary to problem 1, we make no assumptions that the y_k come from one and the same x but rather we consider $n \ll N$ different batches each with their own x_k. Using the these y_k, we solve an unsupervised training problem during which

- n minibatches of observed data, latent, and slack variables are paired into tuples $\{y_i, x_i, z_i\}_{i=1}^n$ with the latent variables z_i's initialized as zero-centered white Gaussian noise, $z_i \sim N(0, I)$. The slack variables x_i's are computed by the numerically expensive Bregman iterations, which during each iteration work on the randomized source experiment of each minibatch.
- latent variables z_i's are sampled from $p(z_i|x_i, w)$ by running l iterations of Stochastic Gradient Langevin Dynamics (SGLD, Welling and Teh [9]) (Equation 7), where w is the current estimate of network weights, and x_i's are computed with Bregman iterations (Equation 8). These iterations for the latent variables are warm-started while keeping the network weights w fixed. This corresponds to an unsupervised inference step where training pairs $\{x_i, z_i\}_{i=1}^n$ are created. Uncertainly in the z_i's is accounted for by SGLD iterations [7, 8].
- the network weights are updated using $\{x_i, z_i\}_{i=1}^n$ with a supervised learning procedure. During this learning step, the network weights are updated by sample averaging the gradients w.r.t. w for all z_i's. As stated by Han et al. [8], we actually compute a Monte Carlo average from these samples.

By following this semi-supervised learning procedure, we expose the generative model to uncertainties in the latent variables by drawing samples from the posterior via Langevin dynamics that involve the following iterations for the pairs $\{x_i,\ z_i\}_{i=1}^n$

$$z_i \leftarrow z_i - \frac{\varepsilon}{2}\nabla_z \left(\lambda^2 \|x_i - g(z_i, w))\|_2^2 + \|z_i\|_2^2\right) + \mathcal{N}(0, \varepsilon I) \tag{7}$$

with ε the steplength. Compared to ordinary gradient descent, 7 contains an additional noise term that under certain conditions allows us to sample from the posterior distribution, $p(z_i|x_i, w)$. The

training samples x_i came from the following Bregman iterations in the outer loop

$$\begin{array}{rcl} \tilde{x}_i & \leftarrow & \tilde{x}_i - t_k \left(A_k^\top (A_k x_i - y_k) + \lambda^2 (x_i - g(z_i, w)) \right) \\ x_i & \leftarrow & \mathcal{P}_{\mathcal{C}}(\tilde{x}_i). \end{array} \tag{8}$$

After sampling the latent variables, we update the network weights via for the z_i's fixed

$$w \leftarrow w - \eta \nabla_w \sum_{i=1}^{n} \|x_i - g(z_i, w)\|_2^2 \tag{9}$$

with η steplength for network weights.

Conceptually, the above training procedure corresponds to carrying out n different inversions for each data set y_i separately. We train the weights of the network as we converge to the different solutions of the Bregman iterations for each dataset. As during Elastic-Averaging Stochastic Gradient Descent [10, Chaudhari et al. [11]], x_i's have room to deviate from each other when λ is not too large. Our approach differs in the sense that we replaced the center variable by a generative network.

5 Example

We numerically conduct a survey where the source experiments contain severe incoherent noise and coherent linearization errors: $e = (F_k(m + \delta m) - F_k(m) - \nabla F_k(m)\delta m)$, where $A_k = \nabla F_k$ is the Jacobian and $F_k(m)$ is the nonlinear forward operator with m the known smooth background model and δm the unknown perturbation (image). The signal-to-noise ratio of the observed data is -11.37 dB. The results of this experiment are included in Figure 1 from which we make the following observations. First, as expected the models generated from $g(z, \widehat{w})$ are smoother than the primal Bregman variable. Second, there are clearly variations amongst the different $g(z, \widehat{w})$'s and these variations average out in the mean, which has fewer imaging artifacts.

Because we were able to train the $g(z, w)$ as a "byproduct" of the inversion, we are able to compute statistical information from the trained generative model that may give us information about the "uncertainty". In Figure 2, we included a plot of the pointwise standard deviation , computed with 3200 random realizations of $g(z, w),\ z \sim p_z(z)$, and two examples of sample "prior" (before training) and "posterior" distribution. As expected, the pointwise standard deviations shows a reasonable sharpening of the probabilities before and after training through inversion. We also argue that the areas of high pointwise standard deviation coincide with regions that are difficult to image because of the linearization error and noise.

6 Discussion and Conclusions

In this work, we tested an inverse problem framework which includes hard constraints and deep priors. Hard constraints are necessary in many problems, such as seismic imaging, where the unknowns must belong to a feasible set in order to ensure the numerical stability of the forward problem. Deep priors, enforced through adherence to the range of a neural network, provide an additional, implicit type of regularization, as demonstrated by recent work [2, Dittmer et al. [3]], and corroborated by our numerical results. The resulting algorithm can be mathematically interpreted in light of expectation maximization methods. Furthermore, connections to elastic averaging SGD [10] highlight potential computational benefits of a parallel (synchronous or asynchronous) implementation.

On a speculative note, we argue that the presented method, which combines stochastic optimization on the dual variable with on-the-fly estimation of the generative model's weights using Langevin dynamics, reaps information on the "posterior" distribution leveraging multiplicity in the data and the fact that the data is acquired over one and the same Earth model. Our preliminary results seem consistent with a behavior to be expected from a "posterior" distribution.

References

[1] Philipp A. Witte, Mathias Louboutin, Fabio Luporini, Gerard J. Gorman, and Felix J. Herrmann. Compressive least-squares migration with on-the-fly fourier transforms. *GEOPHYSICS*, 84(5): R655–R672, 2019. doi: 10.1190/geo2018-0490.1. URL https://doi.org/10.1190/geo2018-0490.1.

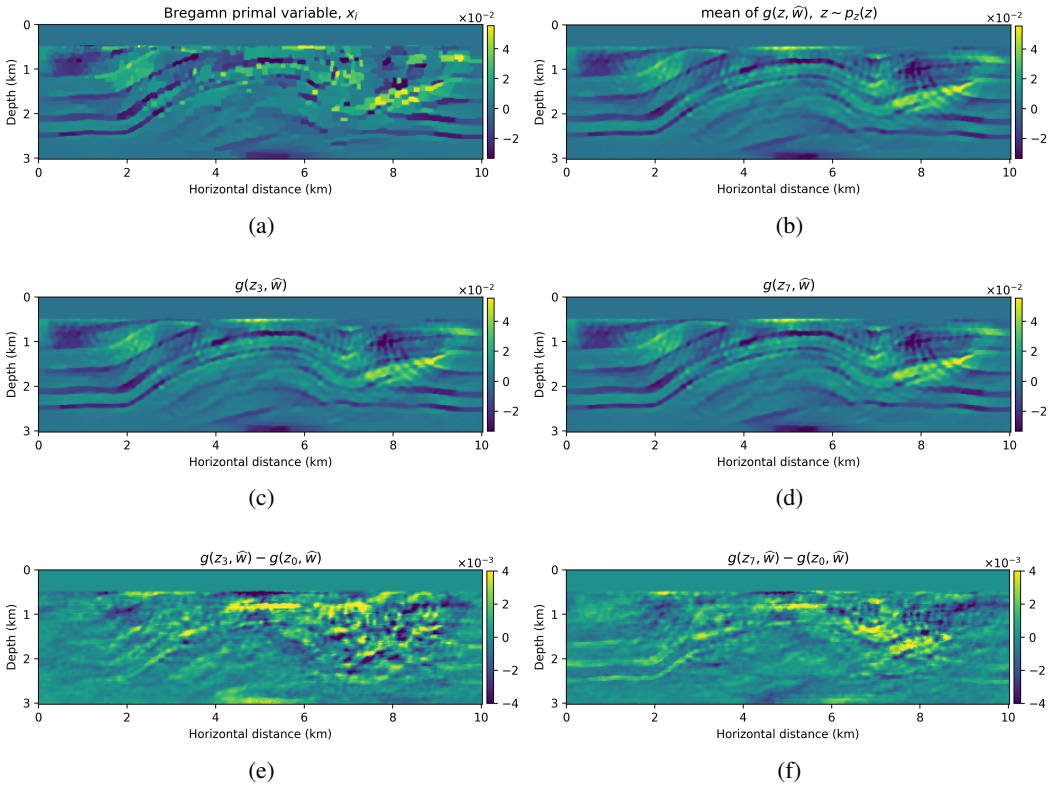

Figure 1: Imaging according to the proposed method. a) a Bregman primal variable x_i^* obtained after 350 Bregman iterations. b) the mean of $g(z, \widehat{w})$ obtained by generating 3200 random realizations of $z \sim p_z(z)$ and averaging the corresponding $g(z, \widehat{w})$'s. c,d) two examples of generated images from $g(z, \widehat{w})$ for different z's. e,f) the differences between images in the middle row with another realization of the network.

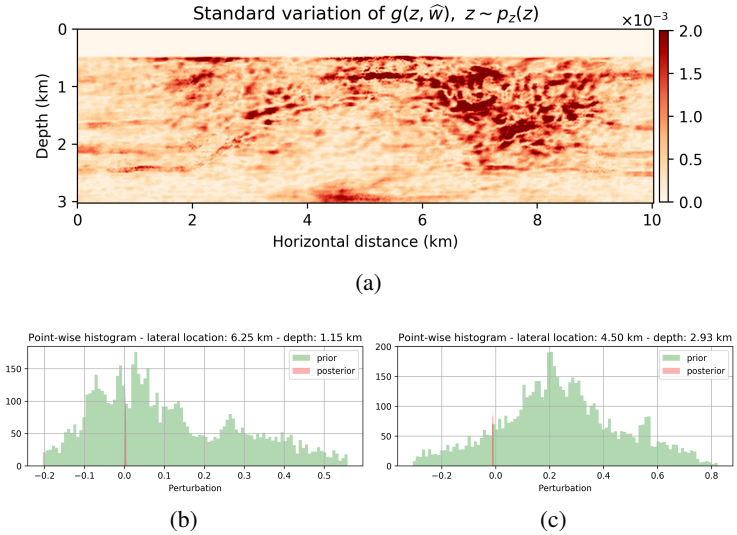

Figure 2: Statistics of imaging according to the proposed method. a) the pointwise standard deviation among samples generated by evaluating $g(z, \widehat{w})$ over 3200 random realizations of $g(z, w),\ z \sim p_z(z)$. b,c) sample "prior" (before training) and "posterior" distribution functions for two points in the model.

[2] Dave Van Veen, Ajil Jalal, Mahdi Soltanolkotabi, Eric Price, Sriram Vishwanath, and Alexandros G. Dimakis. Compressed Sensing with Deep Image Prior and Learned Regularization. *arXiv e-prints*, art. arXiv:1806.06438, Jun 2018.

[3] Sören Dittmer, Tobias Kluth, Peter Maass, and Daniel Otero Baguer. Regularization by architecture: A deep prior approach for inverse problems. *arXiv preprint arXiv:1812.03889*, 2018.

[4] Yulang Wu and George A McMechan. Parametric convolutional neural network-domain full-waveform inversion. *Geophysics*, 84(6):R893–R908, 2019.

[5] Ernie Esser, Lluís Guasch, Tristan van Leeuwen, Aleksandr Y. Aravkin, and Felix J. Herrmann. Total-variation regularization strategies in full-waveform inversion. *SIAM Journal on Imaging Sciences*, 11(1):376–406, 2018. doi: 10.1137/17M111328X. URL https://slim.gatech.edu/Publications/Public/Journals/CoRR/2016/esser2016tvr/esser2016tvr.pdf. (SIAM Journal on Imaging Sciences).

[6] Bas Peters, Brendan R. Smithyman, and Felix J. Herrmann. Projection methods and applications for seismic nonlinear inverse problems with multiple constraints. *Geophysics*, 2018. doi: 10.1190/geo2018-0192.1. URL https://slim.gatech.edu/Publications/Public/Journals/Geophysics/2018/peters2018pmf/peters2018pmf.html. (Published online in Geophysics).

[7] Lukas Mosser, Olivier Dubrule, and M Blunt. Stochastic seismic waveform inversion using generative adversarial networks as a geological prior. In *First EAGE/PESGB Workshop Machine Learning*, 2018.

[8] Tian Han, Yang Lu, Song-Chun Zhu, and Ying Nian Wu. Alternating back-propagation for generator network. In *Thirty-First AAAI Conference on Artificial Intelligence*, 2017.

[9] Max Welling and Yee W Teh. Bayesian learning via stochastic gradient langevin dynamics. In *Proceedings of the 28th international conference on machine learning (ICML-11)*, pages 681–688, 2011.

[10] Sixin Zhang, Anna E Choromanska, and Yann LeCun. Deep learning with elastic averaging sgd. In *Advances in Neural Information Processing Systems*, pages 685–693, 2015.

[11] Pratik Chaudhari, Anna Choromanska, Stefano Soatto, Yann LeCun, Carlo Baldassi, Christian Borgs, Jennifer Chayes, Levent Sagun, and Riccardo Zecchina. Entropy-sgd: Biasing gradient descent into wide valleys. *arXiv preprint arXiv:1611.01838*, 2016.